

# Computations of low-frequency wave loading

X.B. CHEN<sup>1,2</sup> and F. REZENDE<sup>1</sup>

<sup>1</sup>Research Department, BV, 92077 Paris La Défense (France)  
Email: xiao-bo.chen@bureauveritas.com

<sup>2</sup>College of Shipbuilding Engineering, HEU, 150001 Harbin (China)

As the main source of resonant excitations to most offshore moored systems like floating LNG terminals, the low-frequency wave loading is the critical input to motion simulations which are important for the design. Further to the analysis presented by Chen & Duan (2007) on the quadratic transfer function (QTF) of low-frequency wave loading, new developments including numerical results of different components of QTF are presented here. Furthermore, the time-series reconstruction of excitation loads in the motion simulation of mooring systems is analyzed and a new efficient and accurate scheme is demonstrated.

## 1. Formulations of QTF and its approximations

The quadratic transfer function (QTF) of low-frequency wave loads  $\mathbf{F}(\omega_1, \omega_2)$  is composed of two distinct parts : one dependent only on the quadratic products of first-order wave fields and another contributed by the second-order incoming and diffraction potentials.

$$\mathbf{F}(\omega_1, \omega_2) = \mathbf{F}_{\mathbf{q}}(\omega_1, \omega_2) + \mathbf{F}_{\mathbf{p}}(\omega_1, \omega_2) \quad (1)$$

Since the application of low-frequency QTF concerns generally the computation of excitation loading to a moored system whose resonant frequencies are often less than 0.05 rad/s while wave frequencies  $\omega$  are generally larger than 0.30 rad/s, the dynamic behavior of mooring systems is sensitive only to the low-frequency QTF at small values of  $(\omega_1 - \omega_2)$ . In Chen & Duan (2007), it is denoted that

$$\Delta\omega = \omega_1 - \omega_2 \quad \text{and} \quad \omega = (\omega_1 + \omega_2)/2 \quad \text{then} \quad (\omega_1, \omega_2) = (\omega + \Delta\omega/2, \omega - \Delta\omega/2) \quad (2)$$

By assuming  $\Delta\omega \ll 1$ , the quadratic transfer function (QTF) is developed as an expansion :

$$\mathbf{F}(\omega_1, \omega_2) = \mathbf{F}^0(\omega, \omega) + \Delta\omega \mathbf{F}^1(\omega, \omega) + O[(\Delta\omega)^2] \quad (3)$$

with the zeroth-order term contributed by the quadratic products of first-order wave fields and formulated :

$$\mathbf{F}^0 = \mathbf{F}_{\mathbf{q}}^0 = \frac{\rho}{2} \iint_H ds \left[ (\nabla\phi \cdot \nabla\phi^*) \mathbf{n} - \phi_n^* \nabla\phi - \phi_n \nabla\phi^* \right] - \frac{\rho\omega^2}{2g} \oint_{\Gamma} dl (\phi\phi^*) \mathbf{n} \quad (4)$$

as integration over the hull  $H$  and along the waterline  $\Gamma$  in their mean position. In (4),  $\phi$  stands for the first-order velocity potential and  $\phi_n = \nabla\phi \cdot \mathbf{n}$  the normal derivative of  $\phi$  on  $H$ . The superscript \* indicates the complex conjugate. The expression (4) shows that  $\mathbf{F}^0$  is a pure real function dependent on the wave frequency  $\omega$ , which is nothing else than the formulation of drift loads (with a factor 2 of that usually used due to the convention here).

The  $O(\Delta\omega)$  order term in (3) is composed of four components :

$$\mathbf{F}^1 = \mathbf{F}_{\mathbf{q}}^1 + \mathbf{F}_{\mathbf{p}1}^1 + \mathbf{F}_{\mathbf{p}2}^1 + \mathbf{F}_{\mathbf{p}3}^1 \quad (5)$$

with one due to first-order wave fields :

$$\mathbf{F}_{\mathbf{q}}^1 = i\Im \left\{ \frac{\rho}{2} \iint_H ds \left[ (\nabla\varphi \cdot \nabla\varphi^*) \mathbf{n} - (2/\omega) \phi_n^* \nabla\phi - \phi_n^* \nabla\varphi + \varphi_n \nabla\phi^* \right] - \frac{\rho\omega^2}{2g} \oint_{\Gamma} dl (\varphi\phi^*) \mathbf{n} \right\} \quad (6)$$

a pure imaginary function of  $\omega$ . In (6) for  $\mathbf{F}_{\mathbf{q}}^1$ , we have involved the terms  $(\varphi, \nabla\varphi)$  which are defined as the derivative of  $(\phi, \nabla\phi)$  with respect to  $\omega$ . The contribution of second-order incoming waves and diffraction waves of free wave type is given analytically :

$$\mathbf{F}_{\mathbf{p}1}^1 = -i\rho g \forall 4CS(k/\omega) [(1+m_{xx}) \cos \beta + m_{yx} \sin \beta, (1+m_{yy}) \sin \beta + m_{xy} \cos \beta] \quad (7)$$

in which  $\forall$  stands for the buoyant volume,  $C$  and  $S$  dependent on wavenumber  $k$  and waterdepth  $h$  are given in Chen (2006b), while  $(m_{xx}, m_{xy}, m_{yx}, m_{yy})$  added-mass coefficients in double-body flow, dependent only on the hull geometry. To note  $(\beta, k, \omega)$  are wave heading, wavenumber and wave frequency, respectively. The component  $\mathbf{F}_{\mathbf{p}1}^1$  expressed by (7) is pure imaginary dependent on the hull geometry and wave heading.

The component  $\mathbf{F}_{\mathbf{p}2}^1$  is associated with the second-order correction of the boundary condition on  $H$  and written as :

$$\mathbf{F}_{\mathbf{p}2}^1 = -i\rho \iint_H ds \Re\{(i\omega\mathbf{x} - \nabla\phi) \wedge (\mathbf{R}^* \wedge \mathbf{n}) - (\mathbf{x} \cdot \nabla) \nabla\phi^* \cdot \mathbf{n}\} [\psi]^0 \quad (8)$$

with  $(\mathbf{x}, \mathbf{R})$  as the displacement vector and rotation vector, respectively. In (8), the real functions  $[\psi]^0$  are defined as the radiation potentials at zero frequency (double-body flow) associated with the components of the normal vector on  $H$ . Again,  $\mathbf{F}_{\mathbf{p}2}^1$  given by (8) is a pure imaginary function.

Finally, the component representing the effect of forcing pressure over the free surface  $F$  (second-order correction of the boundary condition on  $F$ ) is expressed by :

$$\mathbf{F}_{\mathbf{p}3}^1 = i(\rho\omega/g) \iint_F ds \Im\{\phi \partial_{zz}^2 \phi_P^* + k^2 \phi_P \phi_I^*\} [\psi]^0 \quad (9)$$

in which  $(\phi_P, \phi_I)$  represent the diffraction-radiation potential and incoming wave potential, two components of the first-order potential  $\phi = \phi_I + \phi_P$ .

The second-order low-frequency wave loads  $\mathbf{F}(\omega_1, \omega_2)$  defined by (3) in bichromatic waves of frequencies  $(\omega_1, \omega_2)$  are composed of one component  $\mathbf{F}^0(\omega)$  depending on  $\omega = (\omega_1 + \omega_2)/2$  and another  $\Delta\omega \mathbf{F}^1(\omega)$  linearly proportional to  $\Delta\omega = \omega_1 - \omega_2$ . The striking fact is that  $\mathbf{F}^0(\omega)$  is a pure real function while  $\mathbf{F}^1(\omega)$  a pure imaginary function. The usual approximation proposed by Newman (1974) largely used in practice is based on the use of  $\mathbf{F}^0$  so that it is  $O(1)$  approximation. This study confirms that not only the  $O(1)$  approximation can underestimate largely the second-order wave loads but also it provides wrong phase differences with respect to incoming waves since the complete QTF is a complex function while that by the  $O(1)$  approximation is purely real.

## 2. Time-series reconstruction of low-frequency loading

In irregular waves represented by wave energy spectrum  $S_{\eta\eta}(\omega)$  characterized by the parameters like significant heights, peak periods and form coefficients, the elevation of free surface is written as a Fourier series :

$$\eta(t) = \Re\{E(t)\} \quad \text{with} \quad E(t) = \sum_{j=1}^N a_j \exp(-i\omega_j t) \quad (10)$$

and the complex amplitude :

$$a_j = \exp[ik_j(x \cos \beta + y \sin \beta) + i\epsilon_j] \sqrt{2S_{\eta\eta}(\omega_j) d\omega_j} \quad (11)$$

associated with  $(\omega_j, k_j, \beta, \epsilon_j)$  the wave frequency, wave number, heading and random phase, and dependent on the position  $(x, y)$  with respect to the reference point  $(0, 0)$  and the sampling space  $d\omega_j$  of the spectrum. The low-frequency wave loading in temporal domain is defined by a double summation :

$$F(t) = \Re \left\{ \sum_{i=1}^N \sum_{j=1}^N \mathcal{F}_{ij} a_i a_j^* \exp[-i(\omega_i - \omega_j)t] \right\} \quad (12)$$

with  $a_j^*$  being the complex conjugate of  $a_j$ , and  $\mathcal{F}_{ij} = \mathbf{F}(\omega_i, \omega_j)$  the QTF representing the component in one degree of freedoms or a vector of wave load QTF. At each time step, the low-frequency wave loading is evaluated to perform the time simulation of motions. Due to the double summation, the expression (12) is time-consuming. One approximation largely used in practice is called Newman's approximation in Molin (2002) which is based on :

$$\mathcal{F}_{ij} = \text{sign}(\mathcal{F}) \sqrt{\mathcal{F}_{ii} \cdot \mathcal{F}_{jj}} \quad (13)$$

with  $\text{sign}(\mathcal{F})$  the sign of wave loading which is assumed to remain the same when  $\omega_j$  varies. Introducing (13) into (12), the time-series reconstruction of low-frequency wave loading becomes

$$F(t) = \left| \sum_{j=1}^N \sqrt{\mathcal{F}_{jj}} a_j \exp(-i\omega_j t) \right|^2 \text{sign}(\mathcal{F}) \quad (14)$$

the square of a single summation which is much more economic than the double summation (12).

Considering the fact that

$$\mathbf{F}^{0,1}(\omega, \omega) = [\mathbf{F}^{0,1}(\omega_i, \omega_i) + \mathbf{F}^{0,1}(\omega_j, \omega_j)]/2 + O[(\omega_i - \omega_j)^2] \quad \text{with} \quad \omega = (\omega_i + \omega_j)/2 \quad (15)$$

the approximation (3) can be rewritten as

$$\mathcal{F}_{ij} = (\mathcal{F}_{ii}^0 + \mathcal{F}_{jj}^0)/2 + i(\omega_i - \omega_j)(\mathcal{F}_{ii}^1 + \mathcal{F}_{jj}^1)/2 \quad (16)$$

with  $\mathcal{F}_{jj}^0 = \mathbf{F}^0(\omega_j, \omega_j)$  and  $\mathcal{F}_{jj}^1 = -i\mathbf{F}^1(\omega_j, \omega_j)$  for  $j = 1, 2, \dots, N$  so that both  $\mathcal{F}_{jj}^0$  and  $\mathcal{F}_{jj}^1$  are real functions.

Introducing above expression (16) into (12), the time-series reconstruction of low-frequency wave loading can be obtained by :

$$F(t) = \Re \left\{ \left[ \sum_{j=1}^N \mathcal{F}_{jj}^0 a_j^* \exp(i\omega_j t) \right] E(t) \right\} - \frac{d}{dt} \Re \left\{ \left[ \sum_{j=1}^N \mathcal{F}_{jj}^1 a_j^* \exp(i\omega_j t) \right] E(t) \right\} \quad (17)$$

involving only single summations. The derivative  $d(\cdot)/dt$  in the compact form (17) is understood to apply only to the factor  $\exp(\pm i\omega_j t)$ . The first term in (17) can be considered as the variant of  $O(1)$  approximation of QTF, which is, unlike (14), not restricted by the assumption of a unique sign for QTF.

The new formulation (3) of QTF by the  $O(\Delta\omega)$  approximation provides a novel method to evaluate the low-frequency second-order wave loads in a more accurate than  $O(1)$  approximation and more efficient way comparing to the computation of complete QTF. All the more interesting is that the reconstruction of time series of wave loads is shown to be single summations (17) by using (3) instead of a double summation (12), if the complete QTF (1) is used, to account all pairs of wave interactions which is much more time-consuming.

### 3. Numerical results and discussions

Among components of  $\mathbf{F}^1$  in (3), the component  $\mathbf{F}_{\mathbf{q}}^1$  defined by (6) can be evaluated directly when the terms  $\varphi$  as the derivative of first-order potential with respect to wave frequency are obtained. An indirect way consisting to evaluate the finite difference after having obtained  $\mathbf{F}_{\mathbf{q}}$  for bichromatic waves and drift component  $\mathbf{F}_{\mathbf{q}}^0$  by (4) can be implemented. The term  $\mathbf{F}_{\mathbf{p}1}^1$  defined by (7) depending on the second-order potential of incoming waves and hull geometry can be a dominant one for a body of large volume ( $\nabla$ ) and in water of small depth since  $C \approx (3/4)ka^2/(kh)^3$  for  $kh \rightarrow 0$  as shown in Chen (2006b).  $\mathbf{F}_{\mathbf{p}2}^1$  given by (8) depending on first-order motions is simple and easy to evaluate, negligible for large wavenumber. Finally,  $\mathbf{F}_{\mathbf{p}3}^1$  expressed by (9) is represented by an integral over the free surface which can be performed in a limited area around the body since the integrand decreases rapidly for the radial distance  $R \rightarrow \infty$ , as confirmed by the numerical computations here.

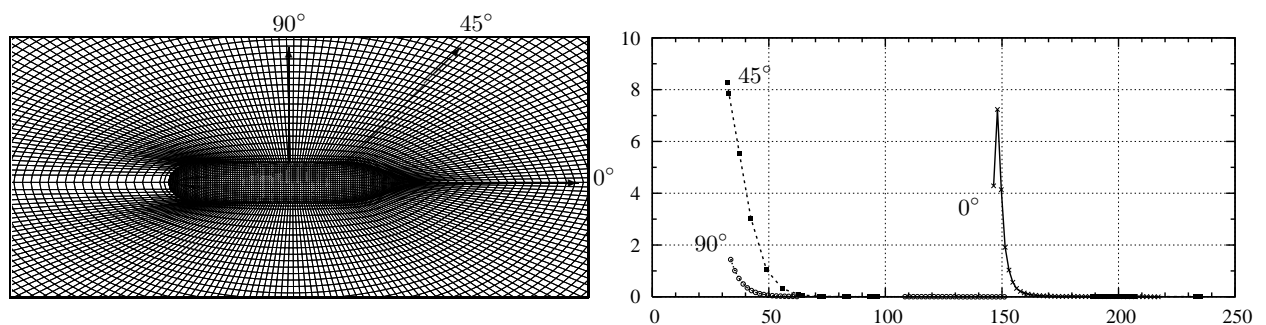


Figure 1: Mesh on LNG hull & the free surface (left) and the integrand of  $\mathbf{F}_{\mathbf{p}3}^1$  (9) in function of radial distances and polar angles (right)

Numerical computations are performed for a standard 138 Km<sup>3</sup> LNG vessel with the main dimensions (length, width and draft) =(274m, 44.2m and 11m), respectively. The half hull is represented by a mesh composed of 2204 planar panels and the area of free surface around the body is meshed in an elliptic form with a ratio of the major axis (along the axis  $\vec{o}\vec{x}$ ) over the minor axis (along the axis  $\vec{o}\vec{y}$ ) equal to 2. About 4000 to 8000 panels are used for a major axis equal to 200m to 500m. A zoom of the hull mesh and the area on the free surface is shown on the left part of Figure 1. Along three radial lines corresponding the polar

angles ( $0^\circ$ ,  $45^\circ$  and  $90^\circ$ ) as indicated on the figure, the integrand of  $\mathbf{F}_{\mathbf{p}3}^1$  (9) is computed for a regular wave of  $\omega = 0.3$  rad/s in water of finite depth (15m), and depicted on the right part of Figure 1. The values of integrand (9) indeed decrease rapidly and  $\mathbf{F}_{\mathbf{p}3}^1$  can be obtained in a relatively easy way. Since the double derivative  $\phi_{Pzz}$  cannot be evaluated with a good accuracy at a point in the vicinity of the waterline, the expression (9) can be transformed into :

$$\mathbf{F}_{\mathbf{p}3}^1 = i(\rho\omega/g)\Im\left\{\iint_F ds \left[ \psi(\phi_x\phi_{Px}^* + \phi_y\phi_{Py}^*) + \phi(\psi_x\phi_{Px}^* + \psi_y\phi_{Py}^*) - k^2\phi_I\phi_P^*\psi \right] + \oint_\Gamma dl \phi\psi(\phi_{Px}^*n_x + \phi_{Py}^*n_y) \right\} \quad (18)$$

by applying Stokes' theorem. In (9), the line  $\Gamma$  includes the waterline and the exterior border of the area  $F$ . The component  $\mathbf{F}_{\mathbf{p}3}^1$  is evaluated in this way and compared with other components.

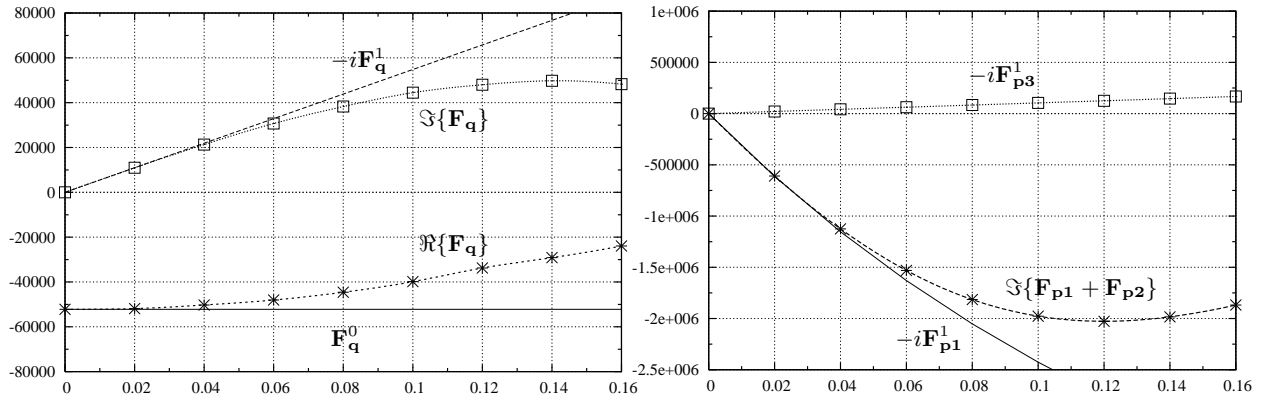


Figure 2: Different components of low-frequency wave loading

The components in (4) and (5) of low-frequency wave load (3) on the LNG vessel are evaluated for a series of wave frequencies associated with  $\omega = 0.3$  rad/s and  $\Delta\omega$  varying from 0 to 0.16 rad/s in water of 15m in depth. They are depicted on Figure 2. The first part dependent on the quadratic products of first-order wave fields is shown on the left while the second part contributed by the second-order incoming and diffraction waves on the right. The real part of QTF includes only  $\mathbf{F}_{\mathbf{q}}^0$  (solid line) which remains constant for all  $\Delta\omega$  and is a very good approximation to the exact values - the real part of  $\mathbf{F}_{\mathbf{q}}$  represented by the cross-dashed line. The imaginary part of QTF contains 4 components. The component  $\mathbf{F}_{\mathbf{q}}^1$  (dashed line) is shown on the left together with the exact values - the imaginary part of  $\mathbf{F}_{\mathbf{q}}$  (square-dashed line). The component  $\mathbf{F}_{\mathbf{p}1}^1$  (dashed line) are depicted on the right with the exact values  $\mathbf{F}_{\mathbf{p}1} + \mathbf{F}_{\mathbf{p}2}$  (cross-dashed line). This indicates that  $\mathbf{F}_{\mathbf{p}2}^1$  is negligible. Finally, the component  $\mathbf{F}_{\mathbf{p}3}^1$  is shown on the right by the square-dashed line.

The quadratic contribution  $\mathbf{F}_{\mathbf{q}}^1$  is positive while the contribution of second-order potentials  $\mathbf{F}_{\mathbf{p}1}^1$  is negative. The component associated with the forcing effect on the free surface  $\mathbf{F}_{\mathbf{p}3}^1$  is small comparing to others. Furthermore, the component  $\mathbf{F}_{\mathbf{p}1}^1$  given by the *analytical* expression (7) is largely dominant for  $\Delta\omega > 0.01$  rad/s. Globally, the  $O(\Delta\omega)$  approximation of QTF is excellent up to  $\Delta\omega = 0.05$  rad/s and still very good for  $\Delta\omega \leq 0.10$  rad/s. The  $O(\Delta\omega)$  approximation of QTF is so believed to give much better values of second-order low-frequency wave loading in an efficient way as described by (17) involving only single summations.

## References

- [1] CHEN X.B. & DUAN W.Y. (2007) Formulation of low-frequency QTF by  $O(\Delta\omega)$  approximation, *Proc 22nd IWWWFB*, Plitvice (Croatia).
- [2] CHEN X.B. (2006a) Middle-field formulation for the computation of wave-drift loads, *J. Engineering Math.* DOI 10.1007/s10665-006-9074-x. **82**, 59:61-82. Published online: Sep 2006.
- [3] MOLIN B. (1979) Second-order diffraction loads upon three-dimensional bodies, *Appl. Ocean Res.*, **1**, 197-202.
- [4] CHEN X.B. (2006b) Set-down in the second-order Stokes' waves, *Proc. 6th Intl Conf. on HydroDynamics*, Ischia (Italy), 179-85.
- [5] NEWMAN J.N. (1974) Second-order, slowly-varying forces on vessels in irregular waves, *Proc. Intl Symp. Dyn. Marine Vehicle & Struc. in Waves*, Mech. Engng. Pub., London (UK), 193-97.
- [6] MOLIN B. (2002) Hydrodynamique des structures offshore *Editions Technip*.